HHS Public Access

Author manuscript

Heart Rhythm. Author manuscript; available in PMC 2022 January 01.

Published in final edited form as:

Heart Rhythm. 2021 January ; 18(1): 98–108. doi:10.1016/j.hrthm.2020.07.036.

Simultaneous activation of the small conductance calcium activated potassium current by acetylcholine and inhibition of sodium current by ajmaline cause J-wave syndrome in Langendorff-perfused rabbit ventricles

Yu-Dong Fei, MD[a,b], **Mu Chen, MD**[a,b], **Shuai Guo, MD**[a], **Akira Ueoka, MD**[a,c], **Zhenhui Chen, PhD**[a], **Michael Rubart-von der Lohe, MD**[d], **Thomas H. Everett IV, PhD, FHRS**[a], **Zhilin Qu, PhD**[e], **James N. Weiss, MD**[e], **Peng-Sheng Chen, MD, FHRS**[a,f]

[a]Krannert Institute of Cardiology, Division of Cardiology, Department of Medicine, Indiana University School of Medicine, Indianapolis, IN, USA

[b]Department of Cardiology, XinHua Hospital affiliated to Shanghai Jiao Tong University School of Medicine, Shanghai, China

[c]Department of Cardiovascular Medicine, Okayama University Graduate School of Medicine, Dentistry, and Pharmaceutical Sciences, Japan

[d]Department of Pediatrics, Riley Heart Research Center, Indiana University School of Medicine, Indianapolis, IN, USA

[e]Department of Medicine (Cardiology) and Physiology, University of California, Los Angeles, CA, USA

[f]Cedars-Sinai Medical Center, Los Angeles, CA, USA

Abstract

Background: Concomitant apamin-sensitive small conductance, calcium activated potassium current (I_{KAS}) activation and I_{Na} inhibition induce J-wave syndrome (JWS) in rabbit hearts. Sudden death in JWS occurs predominantly in men at night, when parasympathetic tone is strong.

Objective: To test the hypotheses that acetylcholine (ACh), the parasympathetic transmitter, activates I_{KAS} and causes JWS in the presence of ajmaline.

Methods: We performed optical mapping in Langendorff-perfused rabbit hearts and whole-cell voltage clamp to determine I_{KAS} in isolated ventricular cardiomyocytes.

Results: ACh (1 μM) + ajmaline (2 μM) induced J-point elevations in all (6 male and 6 female) hearts from 0.01± 0.01 to 0.31 ± 0.05 mV ($p<0.001$), which were reduced by apamin (specific

Correspondence: Peng-Sheng Chen, 8700 Beverly BLVD, Davis 1016, Los Angeles, CA 90048, chenp@cshs.org.

Conflict of interest: None

I_{KAS} inhibitor, 100 nM) to 0.14 ± 0.02 mV (p<0.001). More J-point elevation was noted in males than females (p=0.037). Patch clamp studies showed that ACh significantly (p<0.001) activated I_{KAS} in isolated male but not female ventricular myocytes (n=8). Optical mapping studies showed that ACh induced action potential duration (APD) heterogeneity, which was more significant in right than left ventricles. Apamin in the presence of ACh prolonged both APD_{25} (p<0.001) and APD_{80} (p<0.001), and attenuated APD heterogeneity. Ajmaline further increased APD heterogeneity induced by ACh. Ventricular arrhythmias were induced in 6/6 male and 1/6 female hearts (p= 0.015) in the presence of ACh and ajmaline, which was significantly suppressed by apamin in the former.

Conclusion: ACh activates ventricular I_{KAS}. ACh and ajmaline induce J-wave syndrome and facilitate the induction of ventricular arrhythmias more in male than female ventricles.

Subject codes:

Brugada syndrome; Early repolarization syndrome; Ion Channels; Optical mapping; Ventricular arrhythmias; Sudden cardiac Death

Keywords

J-wave syndrome; ventricular arrhythmia; sex difference; Brugada syndrome; early repolarization syndrome

---

J-wave syndrome (JWS) which includes both the Brugada syndrome and the early repolarization syndrome is characterized by accentuated J-waves on electrocardiogram (ECG) and the vulnerability to life-threatening ventricular arrhythmias.[1] Most patients with JWS are males and the arrhythmias more often occur at night than during the day.[2] In patients with Brugada syndrome, the ventricular tachycardia (VT) / ventricular fibrillation (VF) are mainly initiated from the right ventricle (RV). Epicardial substrate ablation may prevent further arrhythmia episodes in those patients.[3] The development of JWS is attributed to the loss of function of the depolarizing currents (such as I_{Na} or $I_{Ca,L}$) and the concomitant gain of function of the repolarizing currents (such as I_{to}), leading to heterogeneous repolarization.[1] Ajmaline, an I_{Na} blocker, may unmask Brugada syndrome and induce ventricular arrhythmias.[4] The apamin-sensitive small conductance calcium-activated potassium (SK) current (I_{KAS}) is an important repolarization current in the heart.[5, 6] Concomitant I_{KAS} activation and I_{Na} inhibition by cyclohexyl-[2-(3,5-dimethyl-pyrazol-1-yl)-6-methyl-pyrimidin-4-yl]-amine (CyPPA) cause J-point elevation, heterogeneous action potential duration (APD) distribution and spontaneous VT / VF in normal rabbit ventricles.[7] The J-point elevation induced by CyPPA is more prominent in male than in female rabbit ventricles while isoproterenol activates I_{KAS} more significantly in female than in male ventricles.[8] Acetylcholine (ACh) is the parasympathetic neurotransmitter. Concomitant administration of ACh and flecainide caused loss of the canine epicardial action potential (AP) dome with little effect on the endocardial AP, thus giving rise to ST-segment elevation in electrocardiogram (ECG).[9] However, the authors did not report a sex difference in ACh responses or determine whether ACh can activate I_{KAS}.[9] ACh is known to activate I_{KAS} in neurons.[10, 11] We hypothesize that ACh may activate I_{KAS} in the ventricular myocytes and

contribute to the J-point elevation and arrhythmia induction in rabbit ventricles and that these effects are stronger in males than in females.

Methods

Expanded methods can be found in an online supplement.

Optical mapping

Rabbits were euthanized by sodium pentobarbitone overdose (160 mg/kg, i.v.). Hearts were quickly removed and Langendorff perfused with Tyrode's solution (in mmol/L: 128.3 NaCl, 4.7 KCl, 20.2 $NaHCO_3$, 0.4 NaH_2PO_4, 1.2 $MgSO_4$, 11.1 glucose, 1.8 $CaCl_2$) that was kept at 38.3 °C and bubbled with 95% O_2 / 5% CO_2 to maintain a pH of 7.40. PseudoECG was simultaneously recorded by two electrodes placed in the bath close to the right atrium and left ventricular (LV) apex. The signals were bandpass filtered between 1 Hz and 500 Hz. The J point amplitude was the voltage difference between the J point on ECG and the isoelectric segment between the end of P and the onset of R wave (Figure 1). The QRS duration was measured from the onset of the Q wave to the end of S wave or to the peak of the J-wave when J-point was elevated.[12] Optical mapping was performed according to previously reported methods.[7] The hearts remained at sinus rhythm except when RVs were paced for recording of APDs at different pacing cycle lengths (PCLs) and for programmed electrical stimulation to test the inducibility of arrhythmias. APDs at the level of 25% (APD_{25}) and 80% (APD_{80}) repolarization of the action potential were measured. Standard deviation (SD) and range (maximum-minimum) of APD were calculated from the region of interest in the optical maps.

Protocol I: Baseline- ACh- apamin. After baseline measurement, ACh (1 μM) was added to the perfusate. Optical mapping was performed after ACh administration. Cumulatively, apamin (100 nM) was added to the perfusate in the presence of ACh recirculation. Optical maps were performed in the presence of both ACh and apamin.

Protocol II: Baseline- ACh- ajmaline- apamin. After baseline measurement, ACh (1 μM) was added to the perfusate and optical mapping was performed. Cumulatively, ajmaline (2 μM) was added to the perfusate in the presence of ACh. Two programmed electrical stimulation protocols was applied to test the inducibility of ventricular arrhythmias. The first protocol consisted 8 S1 at 600 and 500 ms, followed by S2 and S3 until reaching ventricular effective refractory period or when arrhythmia was induced. The second protocol consisted of trains of paced beats starting from 600 ms with 10-ms decrements. When 1:1 capture was lost, additional train at a cycle length of 5 ms above the last cycle length was used to induce VT or VF. Hearts were electrically defibrillated if VF or VT continued for more than 180 seconds. Finally, apamin (100 nM) was added to the perfusate in the presence of ACh and ajmaline recirculation, and another set of data was collected.

Protocol III: Baseline- ACh- ajmaline- isoproterenol. After baseline measurement, ACh (1 μM) and ajmaline (2 μM) were added to the perfusate. Optical mapping was performed. Isoproterenol (100 nM) was added to the perfusate in the presence of ACh and ajmaline recirculation, and another set of data was collected.

Patch clamp studies

Ventricular cardiomyocytes were isolated as previously described.[13] An Axopatch 200B amplifier and pCLAMP 10 software (Molecular Devices, San Jose, CA) were used to record patch clamp results.

Statistics

Data were shown as mean ± SEM unless otherwise noted. Student's unpaired t tests were used to compare variables between two groups, and paired t test was used to compare between RV and LV of the same heart. Variables of three or more groups were compared by one-way ANOVA with the Bonferroni post hoc analysis. Two-way ANOVA with the Bonferroni post hoc analysis was used to compare variables at different time points. A two-sided P value ≤0.05 was considered statistically significant.

Results

I_{KAS} inhibition attenuated J-point elevation induced by ACh and ajmaline

Ajmaline is a common short-acting sodium channel inhibitor to unmask JWS.[1] ACh elevated J-point in the presence of ajmaline in all of the 12 hearts studied (6 males and 6 females), and specific I_{KAS} inhibition by apamin significantly attenuated J-point elevation ($p<0.001$, Figure 1A). The J-point amplitudes were elevated to 0.31 ± 0.05 mV after ACh and ajmaline from baseline (0.01 ± 0.01 mV), and reduced to 0.14 ± 0.02 mV after adding apamin ($p<0.001$, Figure 1B). J-points were elevated more significantly in males than females (at baseline: 0.01 ± 0.01 vs 0.01 ± 0.01mV; after ACh and ajmaline: 0.41 ± 0.08 vs 0.22 ± 0.03 mV, p=0.037). The ΔJ-point amplitudes induced by ACh and ajmaline were also larger in males than females (0.39 ± 0.07 vs 0.21 ± 0.02 mV, p=0.019). After adding apamin, there was no difference between the J-point amplitudes of males and females (0.16 ± 0.03 vs 0.12 ± 0.02 mV, p=0.316). We also performed a time control study with Tyrode perfusion only. After 40 min of perfusion, J point amplitude remained unchanged (from 0.01 ± 0.05 to 0.01 ± 0.05 mV, p=0.748, Supplemental Figure 1).

The PR intervals were significantly prolonged (ANOVA $p<0.001$). The PR interval was 70.31 ± 1.68 ms at baseline, 90.22 ± 2.63 ms after ACh (p=0.131 vs baseline), 122.75 ± 5.95 ms after ajmaline (p=0.002 vs ACh), and 141.26 ± 12.10 ms after apamin (p=0.193 vs ACh +ajmaline). The QRS durations were also significantly prolonged (ANOVA $p<0.001$). The QRS duration was 58.61 ± 2.45 ms at baseline, 60.49 ± 2.59 ms after ACh (p=1.000 vs baseline), 109.59 ± 7.53 ms after ajmaline ($p<0.001$ vs ACh), and 115.68 ± 7.63 ms after apamin (p=1.000 vs ACh+ajmaline).

ACh activated I_{KAS} in isolated ventricular myocytes

As I_{KAS} inhibition attenuated J-point elevation, we investigated whether I_{KAS} activation by ACh was the underlying mechanism. I_{KAS} was recorded in isolated ventricular myocytes by patch clamping at baseline (Figures 2A & 2B) and in the presence of ACh (Figures 2C & 2D). Males have lower baseline I_{KAS} than females.[8] ACh significantly activated I_{KAS}(ANOVA $p<0.001$ at +20mv, +30mV and +40mV, n=8 in each group, Figure 2E). I_{KAS} increased significantly in male ventricular myocytes in the presence of ACh vs baseline (at

+40mV: 1.508 ± 0.203 vs 0.375 ± 0.054 pA/pF, p<0.001; at +30mV: 1.181 ± 0.123 vs 0.388 ± 0.093 pA/pF, p<0.001; at +20mV: 0.670 ± 0.078 vs 0.268 ± 0.052 pA/pF, p<0.001). The same was not true for female ventricular myocytes (at +40mV: 1.349 ± 0.177 vs 0.823 ± 0.155 pA/pF, p=0.154; at +30mV: 0.932 ± 0.145 vs 0.585 ± 0.056 pA/pF, p=0.196; at +20mV: 0.524 ± 0.074 vs 0.313 ± 0.032 pA/pF, p=0.139). After ACh, I_{KAS} was not significantly different between male and female ventricular myocytes (p=1.000 at +40mV; p=0.706 at +30mV; p=0.643 at +20mV).

ACh activated I_{kas} in rabbit ventricles

Optical mapping (protocol I) was performed to demonstrate the activation of I_{KAS} by ACh at different PCLs in the whole heart. Figure 3A shows representative overlapped V_m traces, APD_{25} and APD_{80} maps. The average APD_{25} and APD_{80} were not significantly changed by ACh. However, APD_{25} distribution showed that the shortening was heterogeneous in the RV (Figures 3A & 4A). After adding apamin, significant prolongation was observed in both APD_{25} (p<0.001 vs ACh at all PCLs) and APD_{80} (p<0.001 vs ACh at all PCLs, Figure 3B).

APD heterogeneity was more significant in RV than LV

Figure 4A shows ΔAPD map of APD_{25} and APD_{80} before and after ACh and before and after apamin. There was significant heterogeneity of ΔAPD_{25}. The ranges of APD_{80} were summarized in Figure 4B. SD was larger in RV than LV (at PCL 350 ms, 7.9±1.5 vs 4.3±0.9 ms, p<0.001; at PCL 300 ms, 7.1±1.2 vs 4.0±1.0 ms, p<0.001; at PCL 280 ms, 6.3±1.3 vs 3.9±1.0 ms, p=0.001; at PCL 250 ms, 6.3±1.0 vs 4.1±0.9 ms, p=0.032). Range of APD_{80} was also larger in RV than LV (at PCL 350 ms, 42.2±8.1 vs 25.2±5.9 ms, p=0.018; at PCL 300 ms, 41.2±7.9 vs 20.4±3.7 ms, p=0.003; at PCL 280 ms, 37.2±7.2 vs 19.8±3.8 ms, p=0.009; at PCL 250 ms, 33.2±4.5 vs 19.8±3.2 ms, p=0.011). There were no significant differences for I_{KAS} in the presence of ACh between male RV and LV cardiomyocytes (at +40 mV, 1.631±0.331 vs 1.459±0.243 pA/pF, p=0.687; at +30 mV, 1.098±0.243 vs 1.107±0.118 pA/pF, p=0.974; at +20 mV, 0.571±0.152 vs 0.605±0.088 pA/pF, p=0.852, Figure 4C). The SD of I_{KAS} in the presence of ACh was larger in RV than LV cardiomyocytes (at +40 mV, 0.741 vs 0.543 pA/pF; at +30 mV, 0.543 vs 0.263 pA/pF; at +20 mV, 0.341 vs 0.197 pA/pF).

I_{KAS} inhibition attenuated JWS induced by ACh and ajmaline

We performed optical mapping (protocol II) to further test the effects of I_{KAS} on JWS. Representative overlapped Vm traces and APD_{80} maps are shown in Figure 5A. While there was no obvious APD heterogeneity at baseline, significant heterogeneity was observed after Ach administration. The APD_{80} at different PCLs are shown in Figure 5B. In spite of increased heterogeneity on the APD_{80} maps in Figure 5A, ACh did not change the overall APD_{80} significantly (p=0.389 at PCL 350ms, p=0.516 at PCL 300ms, p=1.000 at PCL 280ms, p=1.000 at PCL 250ms). Consistent with prior studies,[14] ajmaline prolonged APD_{80} (p<0.001 vs ACh at all PCLs). Apamin further prolonged APD_{80} (p<0.001 vs ACh+ajmaline at PCL 350ms, p<0.001 at PCL 300ms, p<0.001 at PCL 280ms, p=0.011 at PCL 250ms), and reduced heterogeneity of APD distribution.

No spontaneous ventricular arrhythmia was observed in our study. Programmed electrical stimulation was performed to test the inducibility of ventricular arrhythmias at baseline, after ACh and ajmaline, and after adding apamin. Figure 6A shows a representative pseudoECG trace of pacing-induced VT in the presence of ACh and ajmaline. VT/VF was inducible after ACh and ajmaline in 6/6 males and 1/6 females (p=0.015). Of the 7 inducible hearts, 3 of them showed a Torsades de Pointes pattern, and 4 of them showed monomorphic VT. After adding apamin, J-point elevation was suppressed and programmed electrical stimulation failed to induce VT/VF (Figure 6B). VT/VF was inducible in 1/6 males and 0/6 females after adding apamin (Figures 6C), indicating that apamin reduced the inducibility. The V_m traces of beats 1, 2 and 3 of Figure 6A are shown in Figure 6D. Significant differences of APD are present in the RV. The phase maps of beat 3 confirmed the formation of reentry in RV (Figure 6E).

APD heterogeneity was further demonstrated by ΔAPD map, the SD and the range of APD_{80}. Figure 7A showed significant APD_{80} heterogeneity, especially in the RV. SD was significantly increased by ACh and ajmaline compared with baseline ($p<0.001$ at all PCLs), which was significantly attenuated by adding apamin ($p<0.001$ vs ACh+ajmaline at PCL 350ms, p=0.004 at PCL 300ms, p=0.003 at PCL 280ms, p=0.004 at PCL 250ms, Figure 7B). Range of APD_{80} was also significantly increased by ACh and ajmaline ($p<0.001$ vs baseline at all PCLs). Apamin effectively decreased the range of APD_{80} (p=0.006 vs ACh+ajmaline at PCL 350ms, p=0.105 at PCL 300ms, p=0.079 at PCL 280ms, p=0.019 at PCL 250ms, Figure 7C).

As isoproterenol can be used for treatment of Brugada syndrome, we tested the effects of isoproterenol on JWS induced by ACh and ajmaline in two male hearts (Protocol III, Figure 8). Isoproterenol (100 nM) suppressed J-point elevation induced by ACh and ajmaline in both hearts (from 0.2478 mV to 0.1431 mV and from 0.1956 mV to 0.0650 mV, Figure 8A). APD_{80} maps during sinus rhythm are shown in Figure 8B, the AP traces of the 3 locations in Figure 8B are shown in Figure 8C, and ΔAPD maps are shown in Figure 8D. ACh and ajmaline induced significant APD heterogeneity. Adding isoproterenol accelerated the heart rate, shortened APD and attenuated APD heterogeneity.

Discussion

Sex differences and nocturnal sudden death

The JWS is characterized both by a sex difference (male dominance) and nocturnal occurrence of ventricular arrhythmias. The present study and the study by Chen et al[8] point to the possibility that circadian variations of autonomic tone are in part responsible for JWS. The density of I_{KAS} in rabbits is higher on the epicardium than the endocardium.[15] The rabbit ventricular myocytes show spike and dome morphology at slow rates.[16] I_{KAS} activation may promote the loss of AP dome on the epicardium but not endocardium, leading to transmural AP heterogeneity to cause J-point elevation.[17] High sympathetic tone activates I_{KAS} in females during day time but also simultaneously activates $I_{Ca,L}$ to counterbalance its effects on AP dome. Therefore, females are protected against JWS during sympathetic activation. Males are less liable to JWS during daytime because of absence of I_{KAS} activation by the high sympathetic tone. In contrast, high parasympathetic tone

activates I_{KAS} specifically in males at night, but not other inward currents to counterbalance its effects on the AP dome. The absence of I_{KAS} activation by ACh in females protects them against the ventricular arrhythmias at night. Therefore, males are more likely than females to develop nocturnal ventricular arrhythmias and sudden cardiac death.

ACh activates ventricular I_{KAS}

In our study, we used patch clamping and optical mapping to demonstrate that ACh activated ventricular I_{KAS}. Patch clamping results provided direct evidence of I_{KAS} activation by ACh in isolated ventricular cardiomyocytes. In optical mapping experiments, apamin significantly prolonged both APD_{25} and APD_{80} in the presence of ACh. Because apamin could not significantly prolong APD at baseline in normal rabbit ventricles,[8, 15] these results further support the conclusion that I_{KAS} is activated by ACh in rabbit ventricles. These findings were also consistent with studies showing Ach activated SK current in neurons by promoting extracellular calcium entry.[11] ACh shortens atrial APD by activating acetylcholine-activated potassium current ($I_{K\text{-}ACh}$).[18] But in ventricles, the effect of ACh varies from shortening APD[19, 20] to prolonging APD.[21] Moreover, $I_{K\text{-}ACh}$ inhibition could not significantly prolong ventricular APD[20] even in the presence of ACh.[22] These findings are consistent with the low level of $I_{K\text{-}ACh}$ in the ventricles. Therefore, it is unlikely that $I_{K\text{-}ACh}$ activation is responsible for the results in our study.

Our results showed that both PR intervals and QRS durations were significantly prolonged by ajmaline but not affected by ACh or apamin. ACh is known to slow the atrioventricular conduction and prolong the PR interval.[23] We observed a trend of PR interval prolongation induced by ACh, but the changes were statistically insignificant. Ajmaline interacts with multiple ion channels.[14] The final effect was to prolong both the PR interval and QRS duration.[24, 25] Our results are consistent with those studies.

Heterogeneous epicardial I_{KAS} activation

Mantravadi et al[26] showed increased dispersion of repolarization in rabbit ventricles during acetylcholine infusion and during vagal nerve stimulation. The authors proposed that the heterogeneous parasympathetic nerve distribution (base > apex) might play a role in these changes.[27] We did not perform vagal nerve stimulation in the present study. The ACh induced APD heterogeneity in the present study is probably in part related to the heterogeneous upregulation of I_{KAS}. There is a transmural heterogeneity of I_{KAS} distribution in patch clamp studies.[15] Similar to Ach, isoproterenol[8] also causes heterogeneous activation of I_{KAS} on the epicardium. The heterogeneity of APD is greater in RV than in LV. Similar findings were observed in CyPPA-induced JWS.[7] In some regions, the excessive activation of I_{KAS} counterbalances the APD-prolonging effects of Ca^{2+} influx, resulting in short APDs. While in other regions, I_{KAS} activation drives the membrane voltage into the window with delayed $I_{Ca,L}$ inactivation, leading to prolonged APDs. Previous studies showed that the density of I_{to} is markedly higher in RV than LV, which may contribute to the higher risk of formation of re-entries and arrhythmias.[28, 29] That important finding has led to the clinical use of quinidine, an I_{to} blocker, in managing patients with JWS.[1] Because very little I_{to} is present in rabbit ventricles at the physiological heart rate, I_{KAS} plays an important role in phase 1 repolarization in rabbit ventricles. In humans and dogs, I_{to} activation during phase 1

of AP increases the driving force of Ca^{2+} entry through $I_{Ca,L}$ which is a major mechanism of I_{KAS} activation.[30] It is possible that I_{KAS} activation can amplify the I_{to} and play an important role in phase 1 repolarization in humans and dogs. These data also suggest that I_{KAS} blocker, such as ondansetron,[31] may be clinically useful in managing JWS when quinidine is not available or not tolerated.

Limitations of the study

The electrophysiological properties and ion channel expressions were different between species. Rabbit hearts are suitable for investigating cardiac electrophysiology and mechanisms of ventricular arrhythmias,[32] but further translational researches are needed to determine the roles of I_{KAS} in human JWS. A second limitation is that no spontaneous ventricular arrhythmia was observed in our study. It is likely that additional factors are needed to trigger nocturnal sudden cardiac death in JWS.

Conclusions

We conclude that the parasympathetic transmitter ACh activates I_{KAS}. ACh and ajmaline induce J-point elevation and facilitate the induction of ventricular arrhythmias more in male than female ventricles. These findings may in part explain the nocturnal occurrences of ventricular arrhythmias and JWS in males and point to the possible clinical benefit of I_{KAS} blockade in managing patients with JWS.

Supplementary Material

Refer to Web version on PubMed Central for supplementary material.

Acknowledgments

Sources of Funding

This work was supported by National Institutes of Health (grant numbers R01 HL139829, R42DA043391, TR002208-01 and 1OT2OD028190), the American Heart Association (grant number 18TPA34170284 to Dr. Zhenhui Chen), the Dr. Charles Fisch Cardiovascular Research Award endowed by Dr. Suzanne B. Knoebel of the Krannert Institute of Cardiology to Drs Yu-Dong Fei, Shuai Guo and Thomas Everett and the China Scholarship Council to Yu-Dong Fei.

References

1. Antzelevitch C, Yan GX, Ackerman MJ, et al. J-Wave syndromes expert consensus conference report: Emerging concepts and gaps in knowledge. Heart Rhythm 10 2016;13:e295–324. [PubMed: 27423412]
2. Milman A, Andorin A, Postema PG, et al. Ethnic differences in patients with Brugada syndrome and arrhythmic events: New insights from SABRUS. Heart Rhythm 7 5 2019.
3. Nademanee K, Hocini M, Haissaguerre M. Epicardial substrate ablation for Brugada syndrome. Heart Rhythm 3 2017;14:457–461. [PubMed: 27979714]
4. Rolf S, Bruns HJ, Wichter T, et al. The ajmaline challenge in Brugada syndrome: diagnostic impact, safety, and recommended protocol. Eur Heart J 6 2003;24:1104–1112. [PubMed: 12804924]
5. Xu Y, Tuteja D, Zhang Z, et al. Molecular identification and functional roles of a Ca(2+)-activated K + channel in human and mouse hearts. J Biol Chem 2003;278:49085–49094. [PubMed: 13679367]
6. Chang PC, Chen PS. SK channels and ventricular arrhythmias in heart failure. Trends Cardiovasc Med 8 2015;25:508–514. [PubMed: 25743622]

7. Chen M, Xu DZ, Wu AZ, et al. Concomitant SK current activation and sodium current inhibition cause J wave syndrome. JCI Insight 11 15 2018;3:e122329.
8. Chen M, Yin D, Guo S, et al. Sex-Specific Activation of SK Current by Isoproterenol Facilitates Action Potential Triangulation and Arrhythmogenesis in Rabbit Ventricles. The Journal of physiology 6 19 2018;596:4299–4322. [PubMed: 29917243]
9. Yan GX, Antzelevitch C. Cellular basis for the Brugada syndrome and other mechanisms of arrhythmogenesis associated with ST-segment elevation. Circulation 1999;100:1660–1666. [PubMed: 10517739]
10. Parks XX, Contini D, Jordan PM, Holt JC. Confirming a Role for alpha9nAChRs and SK Potassium Channels in Type II Hair Cells of the Turtle Posterior Crista. Front Cell Neurosci 2017;11:356. [PubMed: 29200999]
11. Dasari S, Hill C, Gulledge AT. A unifying hypothesis for M1 muscarinic receptor signalling in pyramidal neurons. The Journal of physiology 3 1 2017;595:1711–1723. [PubMed: 27861914]
12. Shimeno K, Takagi M, Maeda K, et al. A predictor of positive drug provocation testing in individuals with saddle-back type ST-segment elevation. Circ J 10 2009;73:1836–1840. [PubMed: 19734691]
13. Fei YD, Li W, Hou JW, et al. Oxidative Stress-Induced Afterdepolarizations and Protein Kinase C Signaling. Int J Mol Sci 3 30 2017;18:688.
14. Bebarova M, Matejovic P, Pasek M, Simurdova M, Simurda J. Effect of ajmaline on action potential and ionic currents in rat ventricular myocytes. Gen Physiol Biophys 9 2005;24:311–325. [PubMed: 16308426]
15. Chua SK, Chang PC, Maruyama M, et al. Small-conductance calcium-activated potassium channel and recurrent ventricular fibrillation in failing rabbit ventricles. Circ Res 2011;108:971–979. [PubMed: 21350217]
16. Fedida D, Giles WR. Regional variations in action potentials and transient outward current in myocytes isolated from rabbit left ventricle. The Journal of physiology 10 1991;442:191–209. [PubMed: 1665856]
17. Yan GX, Antzelevitch C. Cellular basis for the electrocardiographic J wave. Circulation 1996;93:372–379. [PubMed: 8548912]
18. Zang WJ, Chen LN, Yu XJ, et al. Comparison of effects of acetylcholine on electromechanical characteristics in guinea-pig atrium and ventricle. Exp Physiol 1 2005;90:123–130. [PubMed: 15466461]
19. Liang B, Nissen JD, Laursen M, et al. G-protein-coupled inward rectifier potassium current contributes to ventricular repolarization. Cardiovasc Res 1 1 2014; 101:175–184. [PubMed: 24148898]
20. Matsuda T, Takeda K, Ito M, et al. Atria selective prolongation by NIP-142, an antiarrhythmic agent, of refractory period and action potential duration in guinea pig myocardium. J Pharmacol Sci 5 2005;98:33–40. [PubMed: 15879679]
21. Litovsky SH, Antzelevitch C. Differences in the electrophysiological response of canine ventricular subendocardium and subepicardium to acetylcholine and isoproterenol. A direct effect of acetylcholine in ventricular myocardium. Circulation Research 1990;67:615–627. [PubMed: 2397572]
22. Calloe K, Goodrow R, Olesen SP, Antzelevitch C, Cordeiro JM. Tissue-specific effects of acetylcholine in the canine heart. Am J Physiol Heart Circ Physiol 7 1 2013;305:H66–75. [PubMed: 23645460]
23. Roberge FA, Nadeau RA, James TN. The nature of the PR interval. Cardiovasc Res 1 1968;2:19–30. [PubMed: 5645462]
24. Batchvarov VN, Govindan M, Camm AJ, Behr ER. Significance of QRS prolongation during diagnostic ajmaline test in patients with suspected Brugada syndrome. Heart Rhythm 5 2009;6:625–631. [PubMed: 19389649]
25. Bestetti RB, Ramos CP, Figueredo-Silva J, Sales-Neto VN, Oliveira JS. Ability of the electrocardiogram to detect myocardial lesions in isoproterenol induced rat cardiomyopathy. Cardiovasc Res 12 1987;21:916–921. [PubMed: 3331969]

26. Mantravadi R, Gabris B, Liu T, et al. Autonomic nerve stimulation reverses ventricular repolarization sequence in rabbit hearts. Circ Res 4 13 2007;100:e72–80. [PubMed: 17363699]

27. Kawano H, Okada R, Yano K. Histological study on the distribution of autonomic nerves in the human heart. Heart Vessels 3 2003;18:32–39. [PubMed: 12644879]

28. Antzelevitch C, Yan GX. J-wave syndromes: Brugada and early repolarization syndromes. Heart Rhythm 8 2015;12:1852–1866. [PubMed: 25869754]

29. Di Diego JM, Cordeiro JM, Goodrow RJ, et al. Ionic and cellular basis for the predominance of the Brugada syndrome phenotype in males. Circulation 10 08 2002;106:2004–2011. [PubMed: 12370227]

30. Lu L, Zhang Q, Timofeyev V, et al. Molecular coupling of a Ca2+-activated K+ channel to L-type Ca2+ channels via alpha-actinin2. Circ Res 1 5 2007;100:112–120. [PubMed: 17110593]

31. Ko JS, Guo S, Hassel J, et al. Ondansetron Blocks Wildtype and p.F503L Variant Small Conductance Calcium Activated Potassium Channels. Am J Physiol Heart Circ Physiol 4 20 2018;315:H375–H388. [PubMed: 29677462]

32. Panfilov AV. Is heart size a factor in ventricular fibrillation? Or how close are rabbit and human hearts? Heart Rhythm 7 2006;3:862–864. [PubMed: 16818223]

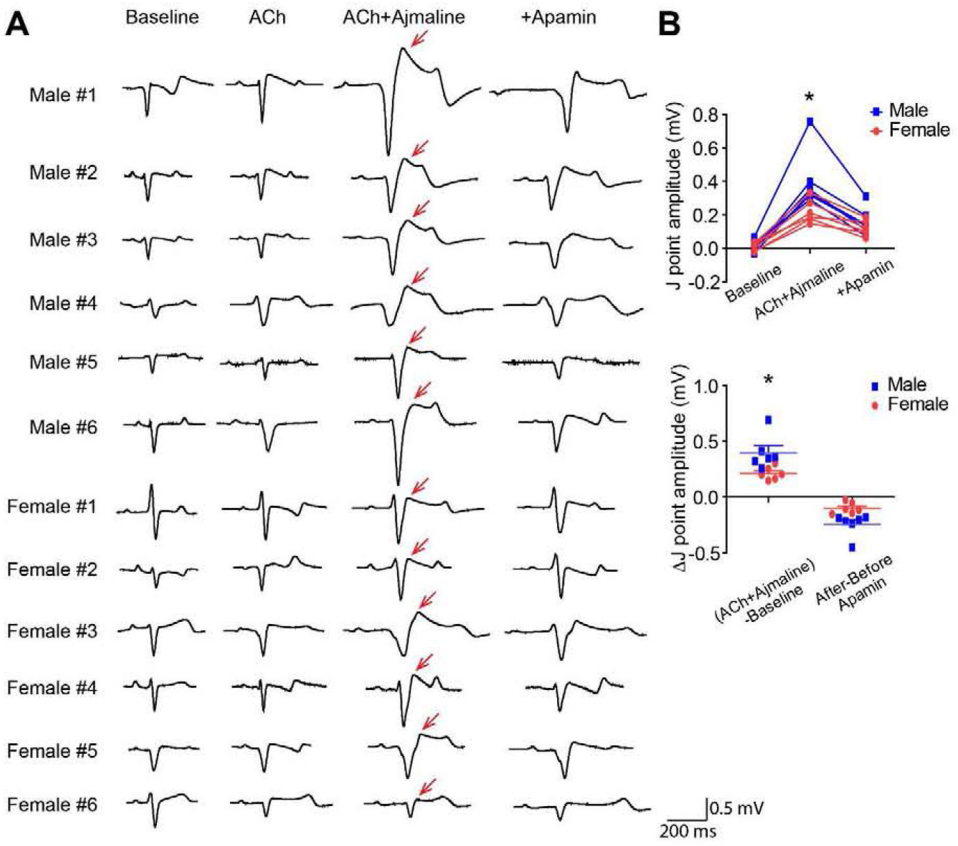

Figure 1.

I_{KAS} inhibition attenuated J-point elevation induced by ACh and ajmaline. (A). PseudoECG during sinus rhythm at baseline, after cumulative addition of ACh, ajmaline and apamin. Red arrows indicate J-point elevation. (B). Summary of J point amplitudes and Δ J point amplitudes in males and females. * $p<0.05$ between male and female.

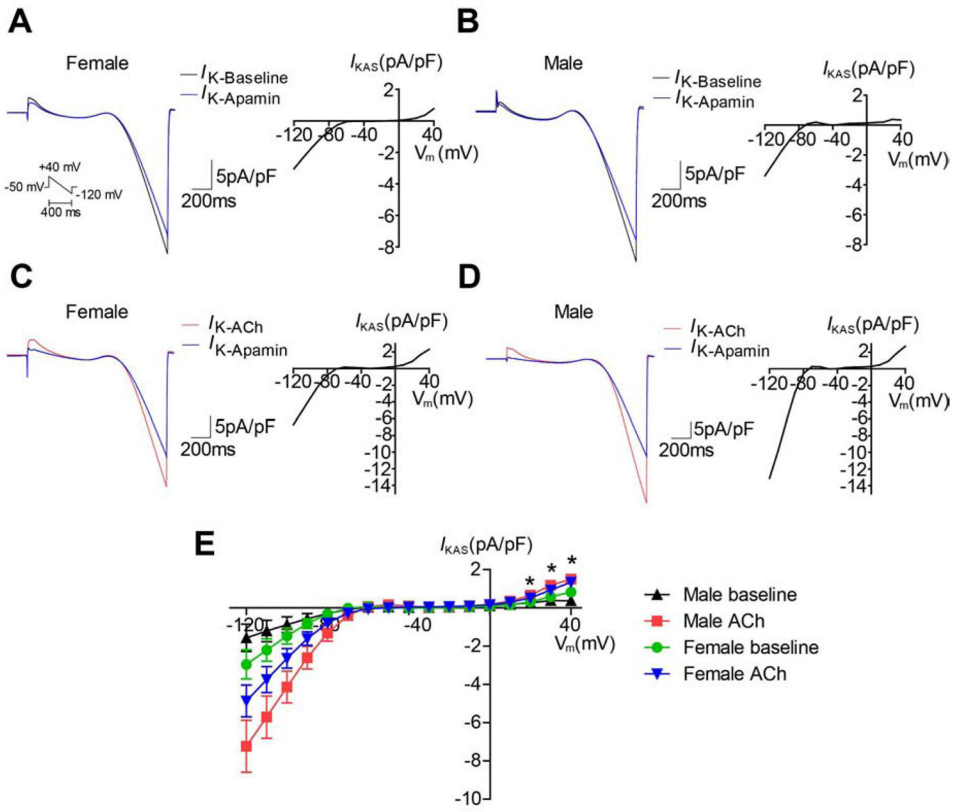

Figure 2.

I_{KAS} was increased in the presence of ACh in isolated ventricular cardiomyocytes. (A-B). Representative current curves (left panel) and I-V curve of I_{KAS} at baseline in female (A) and male (B). (C-D). Representative current curves (left panel) and I-V curve of I_{KAS} in the presence of ACh in female (C) and male (D). (E). Summary of I-V curves. * $p<0.05$ between male baseline and male ACh.

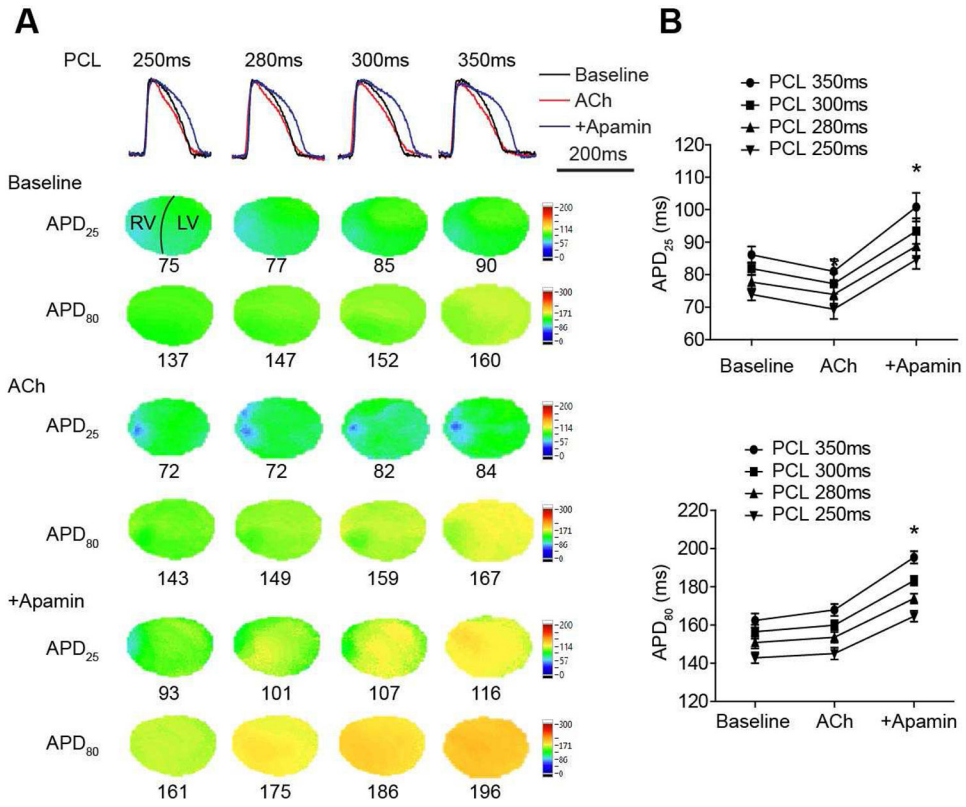

Figure 3.

Effects of ACh and apamin on APD25 and APD_{80} in rabbit ventricles. (A). Overlapped Vm traces and representative APD_{25} and APD_{80} maps in a male ventricle at different PCLs at baseline and after cumulative addition of ACh and apamin. (B). Summary of APD_{25} and APD_{80} at different PCLs (n=12, 6 females and 6 males). * $p<0.05$ before and after apamin.

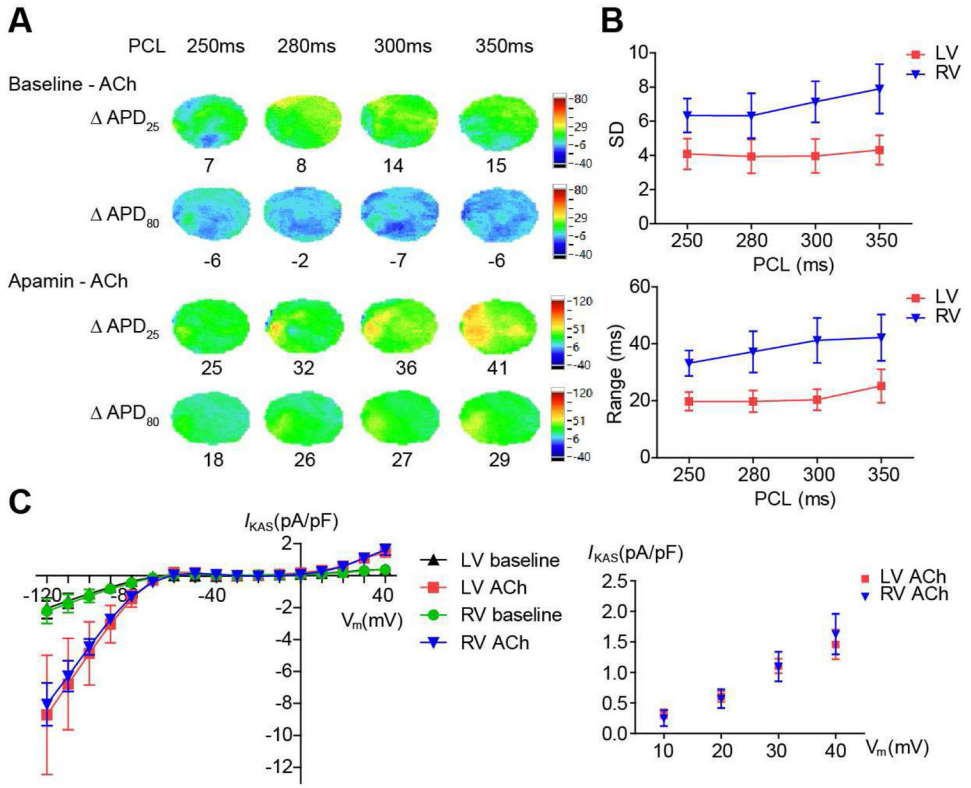

Figure 4.

Heterogeneities of APD and I_{KAS} were larger in RV than LV. (A). Representative ΔAPD_{25} and ΔAPD_{80} maps showing APD heterogeneity. (B). Summary of SD and range (maximum - minimum) of APD_{80} in the presence of ACh (n=12, 6 females and 6 males). (C). Summary of I-V curves of I_{KAS} in male LV and RV cardiomyocytes (left panel) and mean±SEM of I_{KAS} from +10mV to +40 mV (right panel) (n=5 in each group).

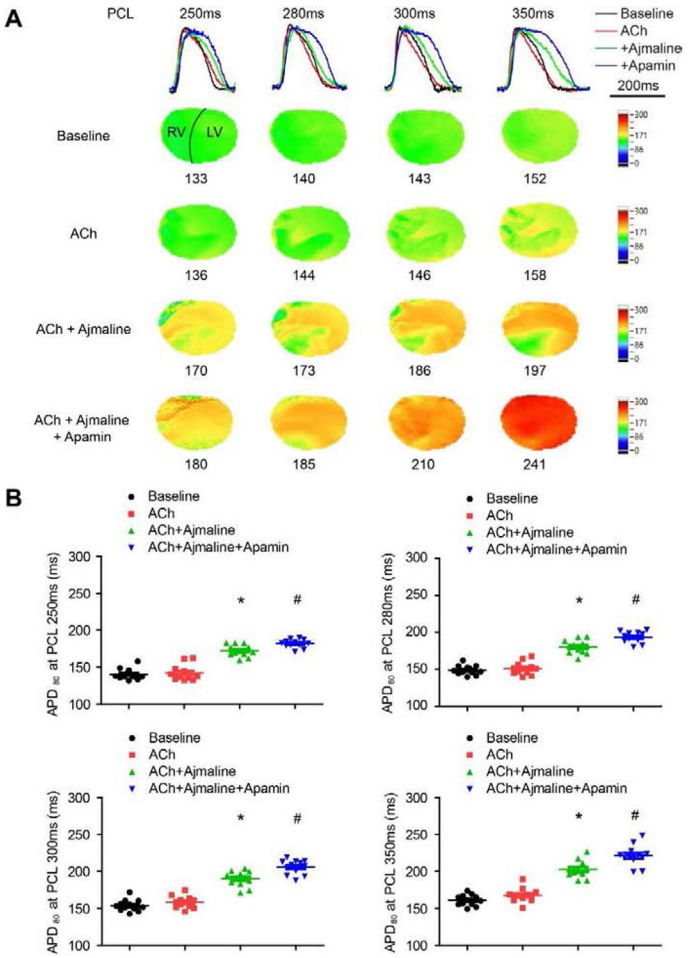

Figure 5.

Effects of ACh, ajmaline and apamin on APD_{80}. (A). Overlapped Vm traces and representative APD_{80} maps at different PCLs at baseline and after cumulative addition of ACh, ajmaline and apamin. (B). Summary of APD_{80} at different PCLs (n=12, 6 females and 6 males). * $p<0.05$ between baseline and ACh+ajmaline. # $p<0.05$ between ACh+ajmaline and ACh+ajmaline+apamin.

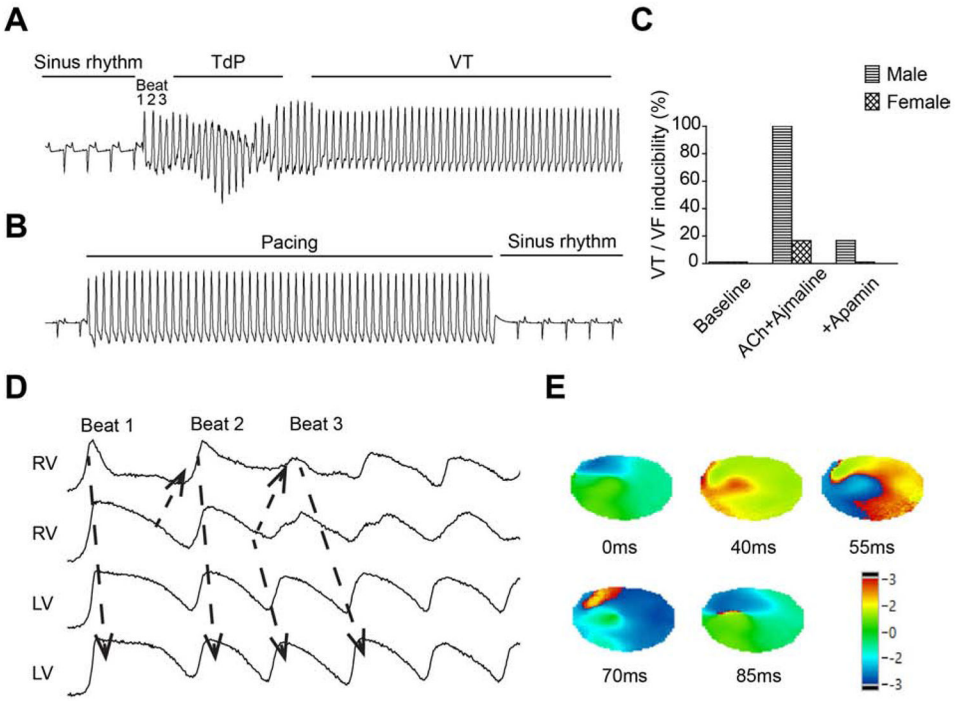

Figure 6.

Ventricular arrhythmias and re-entries were induced by programmed electrical stimulation after ACh and ajmaline, and suppressed by I_{KAS} inhibition. (A). Representative ECG of J-point elevation and pacing-induced arrhythmias in the presence of ACh and ajmaline. (B). Representative ECG after adding apamin showed J-wave suppression and failure to induce VT/VF. (C). Summary of ventricular arrhythmia inducibility. (D). Corresponding Vm traces of beat 1 to beat 3 in (A). (E). Corresponding phase maps of beat 3 in (A). TdP: torsades de pointes.

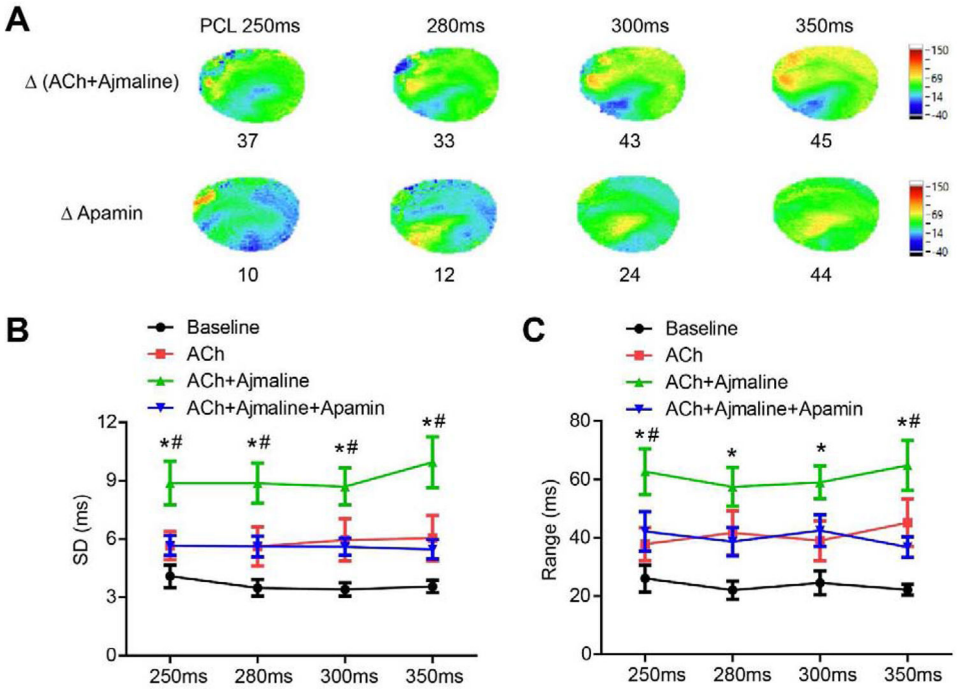

Figure 7.

I_{KAS} inhibition attenuated APD heterogeneity induced by ACh and ajmaline. (A). Representative ΔAPD_{80} maps indicated APD heterogeneity. (B). Summary of SD and range (maximum - minimum) of APD_{80} (n=12, 6 females and 6 males). * $p<0.05$ between baseline and ACh+ajmaline. # $p<0.05$ between ACh+ajmaline and ACh+ajmaline+apamin.

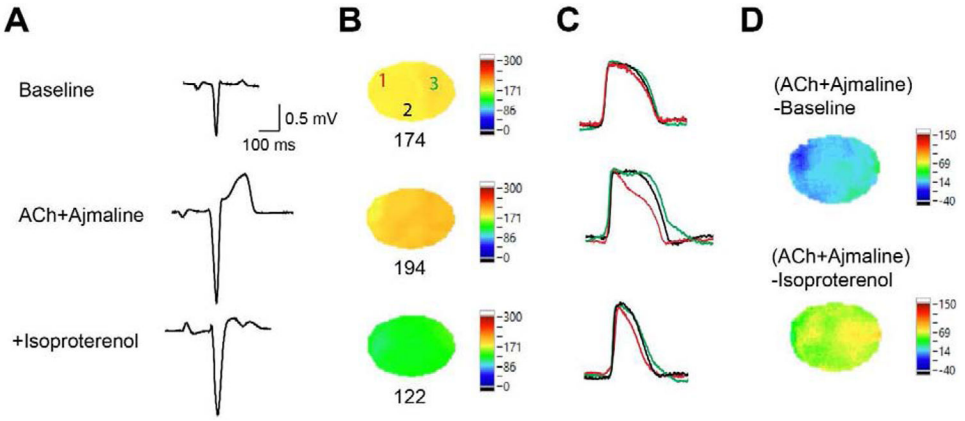

Figure 8.

Isoproterenol attenuated J-point elevation and APD heterogeneity induced by ACh and ajmaline. (A). PseudoECG during sinus rhythm at baseline, after cumulative addition of ACh and ajmaline and isoproterenol. (B). Representative APD_{80} maps at sinus rhythm at baseline, after cumulative addition of ACh and ajmaline and isoproterenol. (C). Corresponding overlapped Vm traces of locations 1 (red), 2 (black) and 3 (green) in (B). (D). ΔAPD_{80} maps before and after ACh+ajmaline and before and after isoproterenol.